Magazine of Civil Engineering

ISSN 2712-8172

journal homepage: http://engstroy.spbstu.ru/

Research article

UDC 624.044

DOI: 10.34910/MCE.116.13

CC BY NC

Elastic-plastic deformation of a round plate reinforced with stiffeners

R.I. Khalmuradov, K. Khudoynazarov ✉, ***U.A. Nishanov***

Samarkand State University, Samarkand, Uzbekistan

✉ *khayrullakhudoynazarov@gmail.com*

Keywords: elastoplasticity, tensor, deformation, nonlinear vibrations, finite deformation, nonlinear equation, reinforce plate

Abstract. The present paper studies the stress-strain state of a round reinforced with stiffeners plate of elastic-plastic material carried out of a refined theory of the type by S.P. Timoshenko It is believed that plate vibrations are excited by a pulsed load. The relationship between displacement and deformation is assumed to be geometrically non-linear. The plate consists of sheathing and rib reinforcement of a quadrangular cross section. The lining materials of the reinforcing ribs are considered identical and obeying Hooke's law. The cross sections of the ribs are constant and are independent of the radial coordinate. The height of the ribs and their locations are set using a single column function. The number of methods of finite differences the solution to the problem. In this case, deformations, forces, moments, and transverse forces are determined at the centers of the grid elements, and displacement and rotation angles are determined at the grid nodes. Given the location of the ribs, the deflection of the central point and the force calculated, depend on the radial co-ordinate and time. Particularly, it was found that the smallest deflection of the central point is achieved when the rib is located in the middle of the radius of the plate; the location of the ribs near the edge of the plate can lead to a decrease in the load-bearing capacity of the structure compared to an un-reinforced plate.

Citation: Khalmuradov, R.I., Khudoynazarov, K., Nishanov, U.A. Elastic-plastic deformation of a round plate reinforced with stiffeners. Magazine of Civil Engineering. 2022. 116(8). Article no. 11613. DOI: 10.34910/MCE.116.13

1. Introduction

Thin elastic structures and their elements are widely used in modern technology and construction. In most cases, these elements operate under the influence of various dynamic loads of a wide range and are in difficult operating conditions [1, 2]. For achieving the desired structural rigidity and increase in strength, its thin-walled part is reinforced with ribs. The ribs increase rigidity, increase the strength of the structure and do not significantly increase the weight of the structure. In addition, the ribs very well transmit forces close to concentrated loads. At the same time, a reduction in the material consumption of structures, beneficial in design. Therefore, in studies of the dynamic nature of plates reinforced by stiffeners, special attention is paid to determining the strength characteristics of plates of increased stiffness under the influence of compressive loads.

The solution to the problems pertaining to the deformation of ribbed plates has been carried out through both analytical and numerical methods. Using analytical methods for calculating plates and shells, supported by stiffeners as other elements of engineering structures, it is possible to calculate their deformed and stressed states with a given or acceptable accuracy.

© Khalmuradov, R.I., Khudoynazarov, K., Nishanov, U.A., 2022. Published by Peter the Great St. Petersburg Polytechnic University.

In mathematical terms, the analytical methods for solving dynamic problems of ribbed plates and shells are complex [3]. Therefore, researchers have tried to overcome these difficulties by limiting the configurations of the ribbed plates and to be content with relatively simple configurations. Due to these difficulties in the scientific literature, till recently, little work has been done using analytical methods of calculation. In article [4] considers a ribbed plate with its structural orthotropy and analyzes its stressed state by analytical, numerical (finite element method) and experimental methods. It has been proved that the reinforcement of the plates with ribs of constant cross-section allows significant reduction of stress in its sections in comparison to an un-supported plate. It has also been noted that the literature on the analytical calculation of the stress-strain state of ribbed plates is quite scanty.

The work [5] is devoted consider shells of a stepped variable thickness when a thickness variation is set by means of unit bar graph functions equal to a difference of two unit functions. It enables for considering ribs, reinforcement plates and cutouts in one structure; a rib and shell contact is arranged along a strip.

In the process of performing dynamic calculations of the elements of structural engineering, the study of their natural vibrations along with the determination of natural frequencies and their natural forms, plays a large role [6, 7]. The same is true for ribbed plates and shells, since the reinforcements change both the spectrum of natural frequencies and the shape of the vibrations [8]. In this direction, one can note articles [9, 10], where the free vibrations of circular and annular plates reinforced on external contours were studied.

Some questions of the dynamic stability of reinforced orthotropic gentle shells of double curvature and viscoelastic flexible plates of variable stiffness under compression were studied in [11, 12]. In the work [11] explored orthotropic shallow shells of double curvature, as well as cylindrical panels that are reinforced from the concave side by an orthogonal grid of stiffeners. The external transverse load acting on the structure is uniformly distributed and has a linear dependency on time. A geometrically nonlinear variant of the model which also takes into account orthotropy of the material and transverse shears are considered. The model is presented as a functional of total deformation energy of the shell. In the paper [12] the dynamic stability of viscoelastic plates of variable stiffness is analyzed. The deflections are described by partial integro-differential equations of motion. The Bubnov–Galerkin method based on monomial and polynomial approximation of deflections is used to reduce the problem to ordinary integro-differential equations with time as an independent variable.

The complexity of analytical calculations forced the authors to limit themselves to a relatively small amount by taking into account the physical and mechanical properties of materials. Therefore, in many studies, numerical methods have been used to solve such problems [13, 14]. For specific ribbed plates, some questions of the numerical calculation of the dispersion curve and the ways to solve them using the finite element method were presented in the scientific work of Finnveden, S. [15]. Based on the obtained analytical, numerical and experimental results, a comparative analysis has been made. The features of wave propagation in directions parallel to the ribs were investigated numerically.

Some problems in solving applied problems using numerical methods, in particular, the finite difference method, for solving the dynamics problems of ribbed rectangular and round plates, plates and shells under the action of pulsed loads were considered in [16–18]. The dynamic behavior of ribbed plates and shells under pulsed loading was also studied by [18]. The effectiveness of the various methods for modeling the influence of reinforcing elements using the generalized Dirac function was analyzed.

A review and some analysis of scientific papers devoted to the method of numerical calculations of various aspects of ribbed structures are available were made in [19] The ideas underlying some numerical developments are related to the spectral finite element or wave methods of finite elements can be viewed in [20]. Numerical calculations of the required parameters are a relatively new and promising area of research into the behavior of ribbed structural elements and, in particular, the plates [21, 22].

The dynamic behavior of a ribbed plate over a surface that moves a linear distributed load studied by [23]. The paper [24], based on the geometrically nonlinear theory of deformation of Mindlin–Reissner shells, analyzes the stress-strain state of shallow shell structures of double curvature, reinforced by the concavity side with a different number of edges.

There have been numerous publications and a continuous expansion of the field of applicability of ribbed plates and shells. However, the problem of formulating more refined models which describe the dynamic processes in them and search for effective analytical methods for solving the corresponding initial-boundary value problems of mathematical physics with allowance for nonlinear properties, such as boarding and ribs, still persists.

Thus, it can be noted that in the study of dynamic processes occurring in ribbed structural elements under the action of pulsed and other fleeting loads, plastic properties are rarely taken into account due to mathematical difficulties. Therefore, to date, a small number of works in the scientific literature have

concerned themselves with the analytical calculation of ribbed plates and shells which take into account the plastic properties of their material.

The present article is devoted to the numerical calculation of a round plate reinforced by a finite number of annular ring stiffeners and also taking into account for the elastoplastic properties of the plate and ribs materials.

2. Methods

2.1. Mathematical model of the problem

In a cylindrical coordinate system (r, φ, z), a round elastoplastic plate is considered, pinched at the edge and reinforced by the ring stiffeners. In this case, the z-axis is directly perpendicular to the plane of the plate. It is believed that the structure consists of a skin and rigidly reinforced ribs to it, the materials of which are the same and obey Hooke's law. The ribs have quadrangular cross sections and are attached to the inner surface of the plate.

A pulsed load $P(t)$ acting on the outer surface of the plate excites oscillations of the plate. The cross sections of the ribs are the same and constant (Fig. 1).

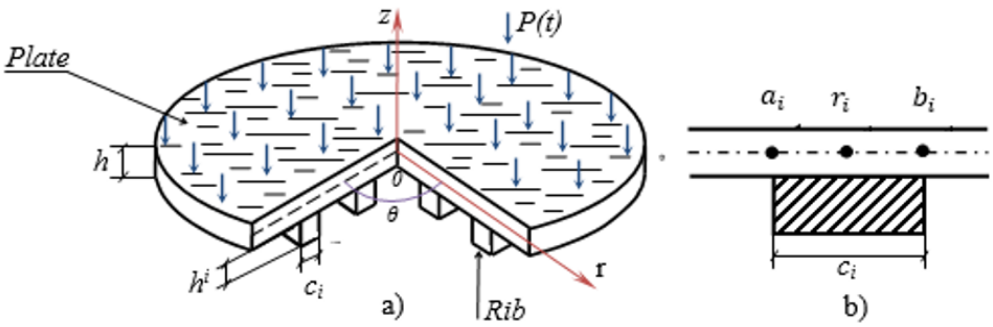

Figure 1. General view of the ribbed plate (*a*) and cross section of the ribs (*b*).

The height of the ribs and their location $H(r_i)$ is determined by using the unit column functions $\delta(r-r_i)$

$$H(r)=\sum_{i=1}^{m} h^i \delta(r-r_i), \quad \delta(r-r_i)=\begin{cases}0, & r<a_i,\ r>b_i,\\ 1, & a_i<r<b_i,\end{cases}$$

Here $a_i = r_i - c/2$; $b_i = r_i + c/2$; r_i - is the coordinate of the midpoint of the contact of the i-th rib and casing; h and c are the height and width of the ribs; m is the number of ribs;

For describing the stress-strain state of the plate, we use the Timoshenko type - nonlinear theory of plate's vibration. Given the asymmetry of the problem, the equations of motion of the plate can be written as follows [1]:

$$(N_1 r)' - N_2 = rp\left[\frac{\partial^2 u}{\partial t^2}(h+F)+\frac{\partial^2 \psi}{\partial t^2}S\right];\ (rQ)' + (N_1 r w')' = r\rho\frac{\partial^2 w}{\partial t^2}(h+F) - rP;$$

$$(rM_1)' - M_2 - rQ = r\rho\left[\frac{\partial^2 \psi}{\partial t^2}\left(\frac{h^3}{12}+J\right)+\frac{\partial^2 u}{\partial t^2}S\right], \tag{1}$$

where ρ is the density of the plate material; h is the thickness of the skin;

$$F=\sum_{i=1}^{m} F^i(r)\delta(r-r_i);\ S=\sum_{i=1}^{m} S^i(r)\delta(r-r_i);\ J=\sum_{i=1}^{m} J^i(r)\delta(r-r_i);$$

$F^i(r)$, $S^i(r)$, $J^i(r)$ are accordingly, the cross-sectional area, the static moment, and the moment of inertia of the section relative to the coordinate axis of the element of the i-rib, with a width equal to unity and height $h^i(r)$ in the section $r = const$; $P(t)$ - is the function of the external load.

Boundary conditions for the structure under consideration:

a) conditions of hard pinching at the edge of the plate: $u = w = \psi = 0$;

b) the conditions of symmetry in the center of the plate: $u = \frac{\partial w}{\partial r} = \psi = 0$ at $r = 0$.

The initial conditions characterizing the state of the plate at $t = 0$ are assumed to be zero, i.e. $u = w = 0$.

2.2. Accounting for plastic deformations

The displacements of an arbitrary point of the normal to the middle surface of the plate with the z coordinate are as in [25]

$$u^z = u + z\psi, \quad w^z = w$$

in accordance with taking into account the axisymmetric loading

$$v^z = v = 0,$$

where u, v, w are the displacements of the points of the middle surface of the plate along the coordinate axes; ψ is the angle of rotation of the normal to the median surface of the plate.

Deformation

$$\varepsilon_1 = \varepsilon_1^0 + z\varepsilon_1^1, \quad \varepsilon_2 = \varepsilon_2^0 + z\varepsilon_2^1$$

are expressed through the displacements u, w and the angle of rotation of the normal to the median surface ψ as follows:

$$\varepsilon_1^0 = \frac{\partial u}{\partial r} + \frac{1}{2}\left(\frac{\partial w}{\partial r}\right)^2, \ \varepsilon_2^0 = \frac{u}{r}, \ \varepsilon_1^1 = \frac{\partial \psi}{\partial r}, \ \varepsilon_2^1 = \frac{\psi}{r}, \ \varepsilon_{13}^0 = \frac{\partial w}{\partial r} + \psi.$$

To describe the dynamic deformation beyond the elastic limit, we use the theory of plastic flow [26]. Focusing on the step-by-step method of solving problems, we divide the loading time into N small, numbered in increasing order of steps. The increment of plastic deformation at step n is denoted by

$$\Delta_n \varepsilon_\alpha^p, \ (n = 1, 2, ..., N; \ \alpha = 1, 2, 13).$$

An algorithm for calculating plastic deformations of a plate is constructed in the light of [26, 27]. First find σ_1 and σ_2. In this case, the values of plastic deformation at the m *-th* step of loading are used. From the stresses thus found, it is possible to determine the stress intensity:

$$\sigma_i^{(\gamma)} = \sqrt{\sigma_1^2 + \sigma_2^2 - \sigma_1\sigma_2},$$

γ is the order of approximation to the strain diagram $\gamma = 1, 2, 3, \ldots$.

If $\sigma_i^{(1)}$ at the considered point of the grid region of the plate for $t > (n+1)\tau$ is less than the value σ_i calculated at step n, then the material is elastically unloaded at the point and we proceed to consider the next node or layer of the grid. Otherwise, we look for the increment $\Delta_{n+1}\varepsilon_l^p$, which is written in the form $\sum_{L=1}^{\gamma} \Delta_{n+1}^L \varepsilon_l^p$, after which we find the following plastic strains

$$\Delta_{n+1}^{\gamma}\varepsilon_1^p = \Delta_{n+1}^{\gamma}\varepsilon_i^p\left(\sigma_1 - \sigma_2/2\right)/\sigma_i^{(\gamma)};\ \Delta_{n+1}^{\gamma}\varepsilon_2^p = \Delta_{n+1}^{\gamma}\varepsilon_i^p\left(\sigma_2 - \sigma_1/2\right)/\sigma_i^{(\gamma)}. \quad (2)$$

Here the increments of plastic deformation are determined from the following relation

$$\Delta_{N+1}^{\gamma}\varepsilon_i^p = \left(1-\frac{E_1}{E}\right)\frac{\sigma_i^{(\gamma)}}{E} - \frac{E_1}{E}\left(\sum_{n=1}^{N}\Delta_n\varepsilon_i^p + \sum_{L=0}^{\gamma-1}\Delta_{N+1}^{L}\varepsilon_i^p\right) - \varepsilon_i^y,$$

where $E_1 = \frac{4}{3}\left(\sigma_P - \sigma_T\right)\frac{100}{\delta}$ is the hardening modulus, σ_T is the yield strength, σ_P is the tensile strength and δ is the residual elongation, which were determined according to the references.

Stresses are found by the stress intensity formula. If in the next iteration, $\sigma_i^{(\gamma)}$ exceeds the diagrammatic stress values at the found level of plastic deformations, the calculations are repeated. The approach to the deformation diagram continues until the stresses σ_1, σ_2 differ from those calculated at the previous iteration by less than 0.5 ... 1.0 MPa, after which the transition of consideration to the next node or time layer takes place, i.e. all calculations are performed before the condition $\left|\Delta_{N+1}^{\gamma}\varepsilon_{rj}^p - \Delta_{N+1}^{\gamma-1}\varepsilon_{rj}^p\right| < \delta$, is satisfied, which provides a sufficient approximation to the deformation diagram.

At the N-th loading step, the total strain ε_i is represented as the sum of the elastic and plastic components

$$\varepsilon_l = \varepsilon_i^y + \sum_{n=1}^{N}\Delta_n\varepsilon_l^p \text{ , here } l = 1,2,3.$$

2.3. Physical equations

The relationship between stress and strain acting at the points of the sheathing and ribs are written as

$$\sigma_1 = \frac{E}{1-\mu^2}\left[\varepsilon_1 + \mu\varepsilon_2 - \sum_{n=1}^{N}\left(\Delta_n\varepsilon_1^p + \mu\Delta_n\varepsilon_2^p\right)\right];$$

$$\sigma_2 = \frac{E}{1-\mu^2}\left[\varepsilon_2 + \mu\varepsilon_1 - \sum_{n=1}^{N}\left(\Delta_n\varepsilon_2^p + \mu\Delta_n\varepsilon_1^p\right)\right];\ \sigma_{13} = \frac{E}{2(1+\mu)}\left[\varepsilon_{13} - \sum_{n=1}^{N}\Delta_n\varepsilon_{13}^p\right]; \quad (3)$$

where $\varepsilon_{13} = f(z)\left(\frac{\partial w}{\partial r} + \psi\right)$; E, μ is the elastic modulus and Poisson's ratio of the material of the lining or ribs [26]; $f(z)$ is a function characterizing the law of the distribution of stresses σ_{13} across the plate thickness: $f(z) = f_0(z)$ for the smooth part; $f(z) = f_1(z)$ at the points where the edges are located:

$$f_0(z) = 6\left[0.25 - \left(\frac{z}{h}\right)^2\right],\ f_1(z) = \frac{3h(h+2H)}{2(h+H)^2}\left(1+2\frac{z}{h}\right)\left[1-2\frac{z}{h+2H}\right],$$

where H is the height of the rib.

The forces, transverse forces and moments per unit length of the section, acting in the section of the plate, reinforced by ribs, have the following form:

$$N_1 = N_1^0 + N_1^R,\ N_2 = N_2^0 + N_2^R,\ M_1 = M_1^0 + M_1^R,\ M_2 = M_2^0 + M_2^R,\ Q = Q^0 + Q^R.$$

The forces, transverse forces and moments related to a smooth plate have the following form [1]:

$$N_1^0 = Eh\left[\varepsilon_1^0 + \mu\varepsilon_2^0 - \frac{1}{1-\mu^2}\sum_{n=1}^{N}\left(\Delta_n^1\varepsilon_1^p + \mu\Delta_n^1\varepsilon_2^p\right)\right];$$

$$N_2^0 = Eh\left[\varepsilon_2^0 + \mu\varepsilon_1^0 - \frac{1}{1-\mu^2}\sum_{n=1}^{N}\left(\Delta_n^1\varepsilon_2^p + \mu\Delta_n^1\varepsilon_1^p\right)\right];$$

$$M_1^0 = D\left[\varepsilon_1^1 + \mu\varepsilon_2^1 - \frac{Eh}{1-\mu^2}\sum_{n=1}^{N}\left(\Delta_n^2\varepsilon_1^p + \mu\Delta_n^2\varepsilon_2^p\right)\right]; \quad (5)$$

$$M_2^0 = D\left[\varepsilon_2^1 + \mu\varepsilon_1^1 - \frac{Eh}{1-\mu^2}\sum_{n=1}^{N}\left(\Delta_n^2\varepsilon_2^p + \mu\Delta_n^2\varepsilon_1^p\right)\right];$$

$$Q^0 = \frac{k^2Eh}{2(1+\mu)}\varepsilon_{13}^0 - \frac{E}{2(1+\mu)}\int_{-h/2}^{h/2} f(z)\sum_{n=1}^{N}\Delta_n\varepsilon_{13}^p dz.$$

Here E, μ are the elastic modulus and Poisson's ratio of the material of a smooth plate

$$D = \frac{Eh^3}{12(1+\mu)};$$

$f(z)$ is a function characterizing the law of stress distribution over the thickness of the structure:

$$\Delta_n^1\varepsilon_l = \frac{1}{h}\int_{-h/2}^{h/2}\Delta_n\varepsilon_l^p dz;\ \Delta_n^2\varepsilon_l = \frac{1}{h}\int_{-h/2}^{h/2}\Delta_n\varepsilon_l^p dz;\ \ l = 1, 2. \quad (6)$$

The forces, moments, and shear forces acting in the sections of the ribs have the following form:

$$N_1^R = \int_{h/2}^{h/2+H}\sigma_1^R dz = A\left(\varepsilon_1^0 + \mu\varepsilon_2^0\right) + B\left(\frac{\partial\psi}{\partial r} + \mu\frac{\psi}{r}\right) - G\sum_{n=1}^{N}\left(\Delta_n^3\varepsilon_1^p + \mu\Delta_n^3\varepsilon_2^p\right);$$

$$N_2^R = \int_{h/2}^{h/2+H}\sigma_2^R dz = A\left(\varepsilon_2^0 + \mu\varepsilon_1^0\right) + B\left(\frac{\psi}{r} + \mu\frac{\partial\psi}{\partial r}\right) - G\sum_{n=1}^{N}\left(\Delta_n^3\varepsilon_2^p + \mu\Delta_n^3\varepsilon_1^p\right);$$

$$M_1^R = \int_{h/2}^{h/2+H}\sigma_1^R z dz = B\left(\varepsilon_1^0 + \mu\varepsilon_2^0\right) + C\left(\frac{\partial\psi}{\partial r} + \mu\frac{\psi}{r}\right) - G\sum_{n=1}^{N}\left(\Delta_n^4\varepsilon_1^p + \mu\Delta_n^4\varepsilon_2^p\right); \quad (7)$$

$$M_2^R = \int_{h/2}^{h/2+H}\sigma_2^R z dz = B\left(\varepsilon_2^0 + \mu\varepsilon_1^0\right) + C\left(\frac{\psi}{r} + \mu\frac{\partial\psi}{\partial r}\right) - G\sum_{n=1}^{N}\left(\Delta_n^4\varepsilon_2^p + \mu\Delta_n^4\varepsilon_1^p\right);$$

$$Q^R = \int_{h/2}^{h/2+H}\sigma_{13}^R dz = D_{13}\left(\frac{\partial w}{\partial r} + \psi\right) - G_{13}\int_{h/2}^{h/2+H} f_1(z)\sum_{n=1}^{N}\Delta_n\varepsilon_{13}^p dz;$$

Here

$$\Delta_n^3\varepsilon_l = \int_{h/2}^{h/2+H}\Delta_n\varepsilon_l^p dz;\ \Delta_n^4\varepsilon_l = \int_{h/2}^{h/2+H}\Delta_n\varepsilon_l^p z dz;\ \ l = 1, 2;\ A = GF;\ B = GS;\ D_{13} = G_{13}H(r);$$

$C = GJ;\ G = \frac{E}{1-\mu^2};\ G_{13} = \frac{k^2E}{2(1+\mu)};\ k^2 = \frac{5}{6};$ $E,\ \mu,\ G$ are elastic constants of the material of the ribs.

2.4. Numerical methods for solving the problem

Below we briefly describe the main points of the finite difference method as applied to the equations of the theory of ribbed plates (1) - (7). The scheme of the numerical solution of the problem by the finite difference method is based on the determination of displacements and rotation angles at the nodes of the grid, and deformations, forces, moments and transverse forces - in the center of the element [27].

The approximation of derivatives in an element has the following form:

$$\left[\frac{\partial f}{\partial r}\right]_{i+1/2} = \frac{f_{i+1} - f_i}{\Delta r_i}, \tag{8}$$

where $\Delta r_i = r_i - r_{i-1}$; f_i is function values in points r_i, $1 \le i \le N+1$.

To approximate the equations of motion (1), which are centered at the nodal points, the central differences are used:

$$\left[\frac{\partial f}{\partial r}\right]_i = \frac{f_{i+1/2} - f_{i-1/2}}{\Delta r_{i+1/2}} \tag{9}$$

non-differentiable terms in equations (1) are reduced to a node by averaging the corresponding values in the elements:

$$f_i = \frac{f_{i+1/2} + f_{i-1/2}}{2}. \tag{10}$$

The time derivatives were approximated by expressions of the form

$$\left[\frac{\partial^2 w}{\partial t^2}\right]_i^n = \frac{w_i^{n+1} - 2w_i^n + w_i^{n-1}}{\tau^2}, \tag{11}$$

where τ is time step, n is index defining the time layer.

The right side of the 1st, 3rd equations of system (1) contains two unknown functions. Therefore, before passing to finite-difference analogues, the 1st and 3rd equations must be solved as a system of algebraic equations for $\frac{\partial^2 u}{\partial t^2}$ and $\frac{\partial^2 \psi}{\partial t^2}$. Then, in differential equations, replace the derivatives with relations of the type (8) - (11).The resulting finite-difference analogue of system (1) has the form

$$u_i^{n+1} = 2u_i^n - u_i^{n-1} + \tau^2 \left\{ \frac{1}{a} U_i^n - \frac{b}{ac - b^2} \left(\psi_i^n - \frac{b}{a} U_i^n \right) \right\};$$

$$w_i^{n+1} = 2w_i^n - w_i^{n-1} + \frac{\tau^2}{a} W_i^n;\ \psi_i^{n+1} = 2\psi_i^n - \psi_i^{n-1} + \frac{\tau^2}{ac - b^2} \left(\Psi_i^n - bU_i^n \right), \tag{12}$$

where $a = \rho(h + F),\ b = \rho S,\ c = \rho(h^3/12 + J)$;

$$U_i^n = \frac{(rN_1)_{i+1/2}^n - (rN_1)_{i-1/2}^n}{\Delta r_{i+1/2} r_{i+1/2}} + \frac{(N_2)_{i+1/2}^n - (N_2)_{i-1/2}^n}{2r_{i+1/2}};$$

$$W_i^n = \frac{(rQ)_{i+1/2}^n - (rQ)_{i-1/2}^n}{\Delta r_{i+1/2} r_{i+1/2}} + \frac{w_i^n - w_{i-1}^n}{\Delta r_i} \frac{1}{\Delta r_{i+1/2}} \frac{(rN_1)_{i+1/2}^n - (rN_1)_{i-1/2}^n}{\Delta r_{i+1/2}} +$$

$$+ \frac{w_{i+1}^n - 2w_i^n - w_{i-1}^n}{(\Delta r_i)^2} \frac{(N_1)_{i+1/2}^n + (N_1)_{i-1/2}^n}{2} + P_{i+1/2}^n;$$

$$\Psi_i^n = \frac{(rM_1)_{i+1/2}^n - (rM_1)_{i-1/2}^n}{\Delta r_{i+1/2} r_{i+1/2}} - \frac{(M_2)_{i+1/2}^n + (M_2)_{i-1/2}^n}{2r_{i+1/2}} - \frac{Q_{i+1/2}^n + Q_{i-1/2}^n}{2}.$$

From relations (2) and (3) we obtain finite-difference expressions for calculating deformations

$$(\varepsilon_1)_{i+1/2}^n = \frac{u_{i+1}^n - u_i^n}{\Delta r_{i+1/2}} + \frac{1}{2} \left(\frac{w_{i+1}^n - w_i^n}{2\Delta r_{i+1/2}} \right)^2;\ (\varepsilon_2)_{i+1/2}^n = \frac{u_{i+1}^n + u_i^n}{2r_{i+1/2}};$$

$$(\varepsilon_{13})_{i+1/2}^n = f(z) \left(\frac{w_{i+1}^n - w_i^n}{\Delta r_{i+1/2}} + \frac{\psi_{i+1}^n + \psi_i^n}{2} \right);\ (\varepsilon_1^z)_{i+1/2}^n = (\varepsilon_1)_{i+1/2}^n + z \frac{\psi_{i+1}^n - \psi_i^n}{\Delta r_{i+1/2}}; \tag{13}$$

$$(\varepsilon_2^z)_{i+1/2}^n = (\varepsilon_2)_{i+1/2}^n + z \frac{\psi_{i+1}^n + \psi_i^n}{2r_{i+1/2}}.$$

The values of stresses, forces, moments and cutting forces are found by formulas (4) - (7), using expressions as in (13).

Formulas of (12) apply only to the internal points of the computational domain. For determining the values of the functions at the boundary points, we use the boundary conditions a) and b) described in the previous section. The hard pinching conditions approximated exactly, and the symmetry conditions are written in finite differences using the following expression:

$$\left[\frac{\partial w}{\partial r}\right]_1^n = \frac{3w_1^n - 4w_2^n + w_3^n}{2\Delta r_2}. \tag{14}$$

The grid functions on two adjacent time layers, necessary to start the calculations, give the initial conditions, from which we obtain equalities of the form

$$w_i^1 = w_i^2 = 0. \tag{15}$$

Using the above equalities, we can find u_i^n, w_i^n, ψ_i^n for any moment of time and any point of the difference grid.

Finite-difference expressions (8) - (12), (14) provide a 2-order approximation. Equalities (15) approximate the initial conditions with the first order of accuracy. The general discrepancy in the approximation of the boundary value problem under consideration by difference relations does not exceed $O(\Delta r^2 + \tau^2)$. When the grid steps tend to zero, the residuals also tend to zero. Therefore, difference equations approximate the original differential equations.

The study of the stability of difference schemes is a difficult task. It is especially difficult to solve for circuits approximating multidimensional nonlinear boundary value problems. The stability of the circuit investigation (12) is studied by numerical experiments. The sighting values of the grid steps ensuring the stability of the calculations found from the Courant condition, are as follows $\tau_1 \le \Delta r / c_1$ here $c_1 = \sqrt{E / \rho(1-\mu^2)}$.

Thus, the solution of differential equations (1) is reduced to calculations using recurrence formulas (12).

3. Results and Discussions

The deflections of the central point of an unreinforced and reinforced by four edges of plates for different values of the amplitude P_0 of the external exponential load are calculated. The results are presented in Figs. 2-4 in the form of graphs according to the deflection *w*and time *t*, and various values of the amplitude of the external exponential load is equal to 2.5; 5; 7.5; 10 MPa.

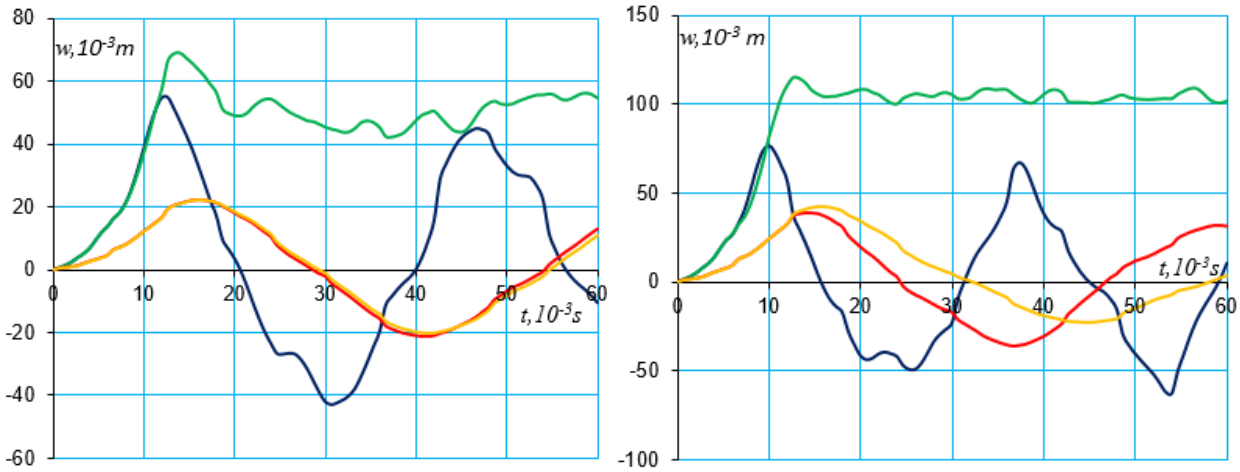

a) **b)**

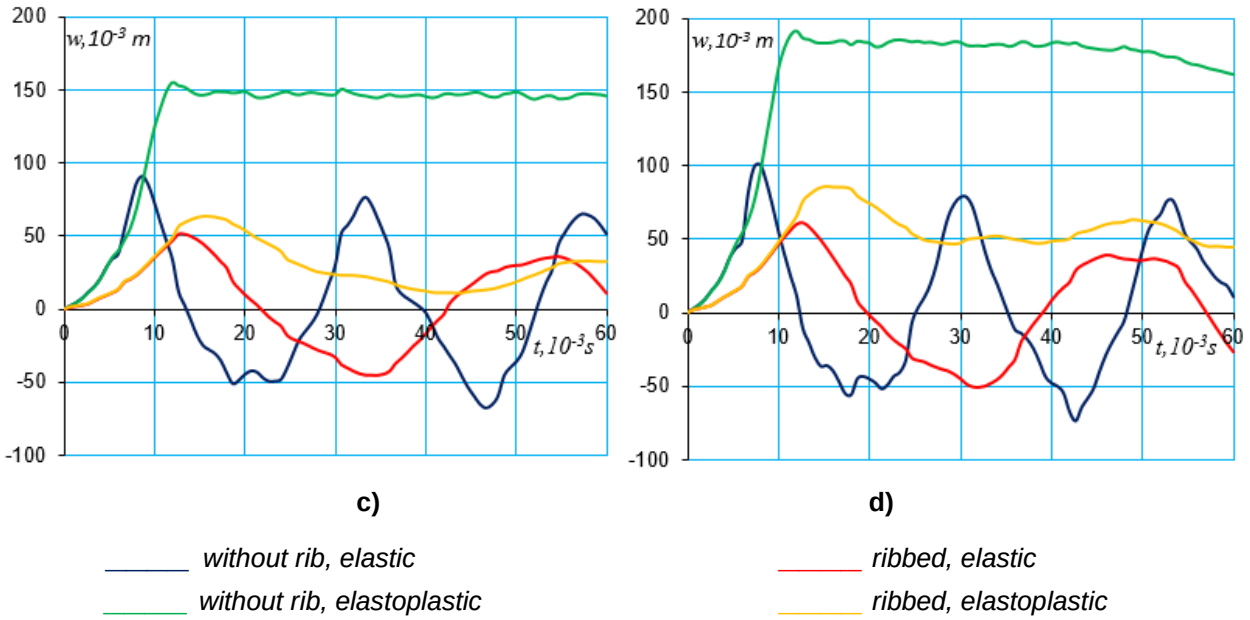

Figure 2. According to the deflection of the central point reinforced by four ribs and unreinforced plates at a)P_0 = 2.5 MPa; b)P_0 = 5 MPa; c)P_0 = 7.5 MPa; d)P_0 = 10 MPa.

Fig. 2,a shows graphs of the deflection of central points reinforced by four ribs and unreinforced plates with an external load amplitude of 2.5MPa. From the graphs presented, it follows that for an unreinforced plate, taking into account plastic deformation, leads to an increase in the deflection values for all time instants. For example, the maximum values of the deflection of the central point calculated by the elastic and elastic-plastic models differ by 32%. In the case when the plate is reinforced by 4 ribs, the graphs of the dependences of the deflection on time, in the elastic and elastic-plastic cases, merge. This shows that under external exponential loads, the amplitudes of which do not exceed 2.5MPa, the influence of plastic deformation can be neglected to calculate the plates reinforced by four edge of the plate. In a particular case, for the elastic model of the plate and stiffening ribs, the results obtained coincide with the analogous results of the work [28].

At an external load with an amplitude of 5MPa and higher, Fig. 2 *b-d*, the effect of plastic deformation on the deflection cannot be neglected. As the results show in Fig. 2 *b-d*, the larger the amplitude of the external load the higher is the deflection obtained by the elastic-plastic model as compared to the elastic model, for example, the maximum value of the elastic-plastic deformation of a smooth plate at P_0 = 2.5MPa is ≈0.068 m; at P_0 = 5MPa it is equal t_0 ≈0.12m; at P_0 = 7.5MPa it is equal t_0 ≈0.151m; and at P_0 = 10MPa it is equal t_0 ≈0.190 m.

With an increase in amplitude of the external load, the difference between the values of deflection of the central point calculated by the elastic and elastic-plastic models increases. For example, for a point in time equal to 0.003 s the specified difference reaches: a) at P_0 = 5 MPa - t_0≈ 0,015 m; b) at P_0 = 7.5 MPa - t_0≈ 0.07 m; c) at P_0 = 10 MPa - t_0≈ 0.098 m.

The graphs of the deflection of the central point of both smooth and reinforced plates, obtained on the basis of the elastic model, for all values of the external load, are pronouncedly sinusoidal in nature. At the same time, the graphs obtained on the basis of the elastic-plastic model, having reached a relative maximum under the action of average load (Fig. 2 b, c), have a straightforward character, with a transition to a slowly descending curve with increasing external load (Fig. 2 *d*).

Fig. 3a) shows graphs of the dependence of the deflection of the central point of the plate on the radial coordinate with an external load amplitude equal to P_0 = 2.5 MPa, calculated by the elastic-plastic model. The cases of non-reinforcement and reinforcement of the plate by one (n = 1), two (n = 2) and four (n = 4) ribs for the time t = 0.0012 s were also considered. The graphs show the effect of reducing deflection by reinforcing the plate with stiffeners, which is 43% for one, 62% for two, and 73% for four reinforcing ribs. From this it follows that the calculation method allows you to achieve the desired value of the deflection by varying the number of ribs.

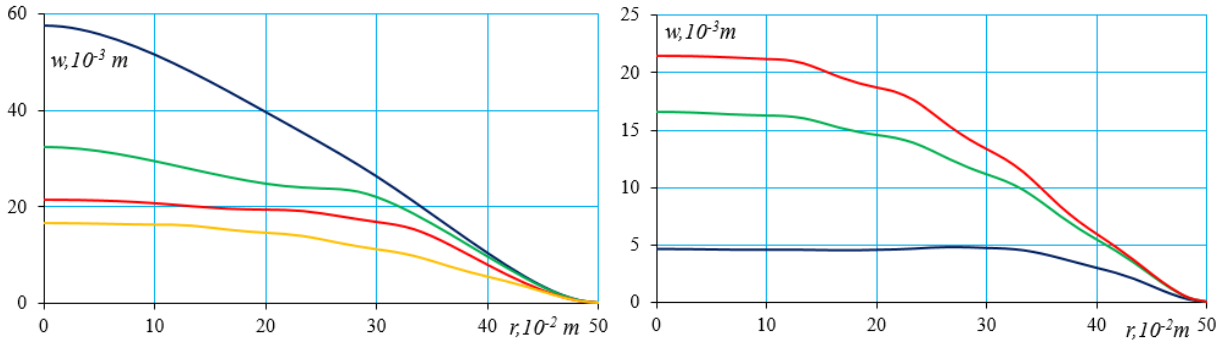

a) b)

Figure 3. According to the deflection on the radial coordinate at P_0 = 2.5MPa *a*)*n* = 1,2,4; *t* = 0.0012 s (____without rib, ____1rib, ____ 2rib, ____4rib); *b*)*n* = 4 (____*t* = 0.0006s,____*t* = 0.0012s, ___*t* = 0.0018s).

Fig. 3b) shows the plots of deflection of the central point reinforced by four (n = 4) plate edge on the radial coordinate at different points in time: t = 0.0006s; 0.0012 s; 0.0018s. Calculations show that with an increase in the duration of the external load, the deflection values increase, for example, the deflection value at the time t = 0.0018 s is four times higher than the value at the time t = 0.0006 s, i.e. with an increase in the action of an external force by three times, the deflection value increases by four times.

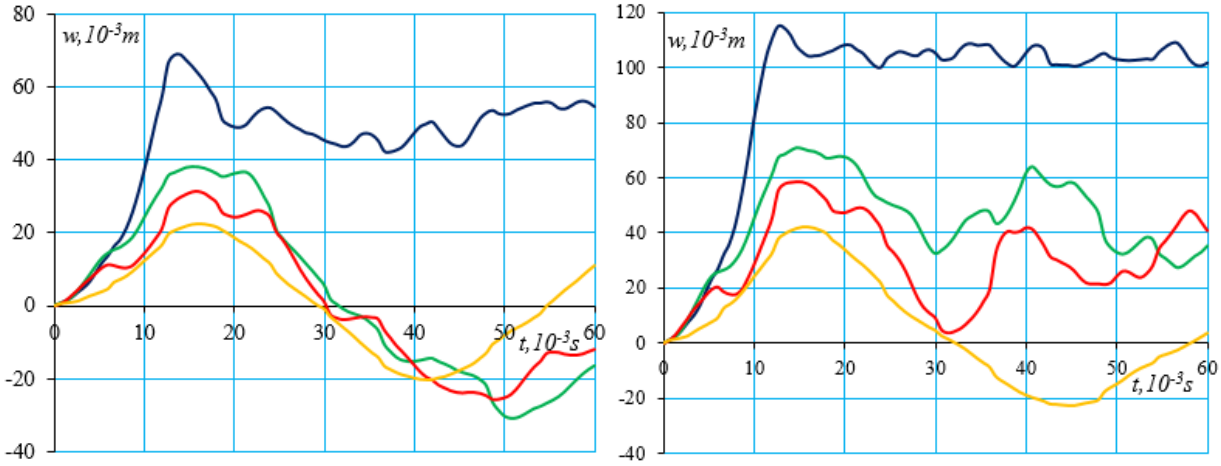

a) b)

Figure 4. According to deflection on time at *n* = 1,2,4: *a*) P_0 = 2.5 MPa; *b*) P_0 = 5 MPa (____without rib, ____1 rib, ____ 2rib, ____4 rib).

Fig. 4 a) and Fig. 4b) show the graphs of deflection of the central point of unreinforced and reinforced by one (n =1), two (n =2) and four (n =4) stiffeners for different external load amplitudes equal to - *a*) at P_0 = 2.5 MPa; and *b*) at P_0 = 5 MPa. The deflection on time in all cases are oscillatory in nature. For an unreinforced plate in both cases of external load, these oscillations, after reaching the maximum value, have relatively small oscillation amplitudes. In reinforced plates this does not occur. Here, the oscillation amplitude is much higher. The difference between the deflection values at the maximum and minimum points in the case of n =1 and P_0 = 2.5 MPa is approximately 0.068 m at P_0 = 5 MPa; and at P_0 = 5 MPa it is equal to 0.032 m etc. A comparison of the dependences in Fig. 4 *a*) and Fig. 4 *b*) shows that with an increase in the amplitude of the external load by a factor of two, in the case of an unsupported plate, the deflection increases by 1.65 times; if there are two reinforcement ribs this indicator decreases by 1.5 times.

The forces and moments in unreinforced and reinforced plates are calculated from the elastic and elastic-plastic models, which confirm the above conclusions. In fact, the proposed elastoplastic model for calculating a reinforced circular plate allows to determine the deflections, forces and moments at arbitrary points of the plate by coordinate and time. Comparative analysis of constitutive relations and the obtained numerical results of calculating the plate deflection by elastic and elastic-plastic models show that the proposed model is a generalization of the elastic model of the work [1] for the case of taking into account the plastic properties of materials of a circular plate and stiffening ribs. In this case, the proposed numerical

method for calculating a reinforced plate based on an elastoplastic model, in the absence of reinforcing stiffening ribs, coincides with the method for calculating elastic-plastic plates proposed in the work [26].

4. Conclusions

The conclusions arrived at in the paper are the following:

- an elastoplastic model for calculating a round discretely finned plate is proposed, which allows one to determine the deflection, forces and moments at the points of the plate.
- the deflections of the central point of an unreinforced and reinforced by four edges of plates for different values of the amplitude P_0 of the external exponential load are calculated. The results are presented in the form of graphs of the dependence of the deflection w and time t for various values of the amplitude of the external exponential load equal to 2.5; 5; 7.5; and 10 MPa;
- -the maximum deflection values of the central point of the plate, calculated by elastic and elastic-plastic models, differ by 32 %. In the case when the plate is supported by 4 ribs, the graphs of the dependences of the deflection on time in the elastic and elastoplastic cases merge. This shows that under external exponential loads, the amplitudes of which do not exceed 2.5 MPa, the influence of plastic deformation can be neglected for calculating the plate, backed by a large number of stiffeners;
- numerical calculations of the deflection, forces, and moments at the points of the fin plate show that the proposed model and calculation method allow us to achieve the desired value of deflection by varying the number of ribs.

References

1. Il'in, V.P., Karpov, V.V. Ustoychivost rebristych obolochek pri bolshich peremesheniyach [Stability of ribbed shells for large displacements]. Leningrad: Stroyizdat, 1986. 168 p. (rus)
2. Karpov, V.V. Prochnost i ustoychivost podkreplennykh obolochek vrasheniya:v 2 chastyach.Chast 1: Modeli i algoritmy issledovaniya prochnostii i ustoychivosti podkreplennykh obolochek vrasheniya [Strength and Stability of Reinforced Shells of Revolution, in 2 parts, Part 1: Modells and Algorithms of Studying the Strength and Stability of Reinforced Shells of Revolution]. Moskov: Fizmatlit, 2010. 288 p. (rus)
3. Karpov, V.V., Semenov, A.A. Mathematical model of deformation of orthotropic reinforced shells of revolution. Magazine of Civil Engineering. 2013. No. 5. Pp. 100–106. DOI: 10.5862/MCE.40.11
4. Popa, C.T., Iatan, R.T., Manescu, C.I. Stress states in plane and ribbed circular plates. Journal Proceedings in Manufacturing Systems. 2013. 8(1). Pp. 53–58.
5. Karpov, V.V. Models of the shells having ribs, reinforcement plates and cutouts. International Journal of Solids and Structures. 2018. 146(1). Pp. 117–135. DOI: 10.1016/j.ijsolstr.2018.03.024Get rights and content
6. Khodzhaev, D., Abdikarimov, R., Vatin, N. Nonlinear oscillations of a viscoelastic cylindrical panel with concentrated masses. MATEC Web of Conferences. EECE-2018. 2018. 245. 01001. DOI: 10.1051/matecconf/201824501001
7. Khudoynazarov, K.K., Burkutboyev, Sh.M. Mathematical modeling of the rotating cylindrical shell torsional vibrations factored in the internal viscous fluid. Matematicheskoe Modelirovanie i Chislennye Metody. 2017. No. 16. Pp. 31–47. DOI: 10.18698/2309-3684-2017-4-3147
8. Ichchou, M.N., Berthaut, J., Collet, M. Accepted for publication. Multi-mode wave propagation in ribbed plates, Part II, Predictions and comparisons. International Journal of Solids and Structures. 2008. 45(5). Pp. 1196–1216. DOI: 10.1016/j.ijsolstr.2007.08.020
9. Stuart, R. J., Carney, J.F. Vibration of edge reinforced annular plates. Journal of Sound and Vibration. 1974. 35(1). Pp. 23–33.
10. Stuart, R.J., Sarney, J.F. Vibration of annular plates with edge-beams. Journal AIAA. 1974. 12(1). Pp. 5–6.
11. Semenov, A.A. Dynamic buckling of stiffened orthotropic shell structures. Magazine of Civil Engineering. 2018. 82(6). Pp. 3–11. DOI: 10.18720/MCE.82.1
12. Abdikarimov,R.A., Khudayarov, B.A. Dynamic stability of viscoelastic flexible plates of variable stiffness under axial compression. International Applied Mechanics, New York. 2014. Vol. 50. No. 4. Pp. 389–398. DOI: 10.1007/s10778-014-0642-x
13. Popa C., Anghelina F.V., Despa V. Finite element and experimental analysis of stresses state for circular plates. IOP Conf.Series: Materials Science and Engineering. 444. 062019. 2018. DOI: 10.1088/1757-899X/444/6/062019.
14. Khudayarov, B.A., Ruzmetov, K., Turaev, F., Vakhobov, V., Khidoyatova, M., Mirzaev S.S., Abdikarimov, R. Numerical modeling of nonlinear vibrations of viscoelastic shallow shells. Engineering Solid Mechanics. 2020. 8(3). Pp. 199–204.
15. Finnveden, S. Spectral finite element analysis of the vibration of straight fluid-filled pipes with flanges. J. of Sound and Vibration. 1996. 199(1). Pp. 125–154. DOI: 10.1006/jsvi.1996.0602
16. Khodzhaev, D.A., Abdikarimov, R.A., Mirsaidov, M.M. Dynamics of a physically nonlinear viscoelastic cylindrical shell with a concentrated mass. Magazine of Civil Engineering. 2019. 91(7). Pp. 39–48. DOI: 10.18720//MCE.91.4
17. Loh, H.C., Carney, J.F. Vibration and Stability of Spinning Annular Plates Reinforced With Edge Beams. Journal ofAppliedMechanics. 1997.44(3). Pp. 499–501.
18. Galiev, Sh.U., Karshiev, A.B. Chislenniy analiz tochnosti modeley rebristogo spheric heskogo kupola, podverjennogo impulsnomu nagrujeniyu [Numerical analysis of the accuracy of models of a ribbed spherical dome subject to pulsed loading]. Problemi prochnosti. 1990. No. 5. Pp. 83–86. (rus)
19. Banerjee, S., Kundu, T. Elastic wave propagation in sinusoidally corrugated waveguides. Journal of Acoustical Society of America. 2006. 119 (4). Pp. 2006–2017. DOI: 10.1121/1.2172170
20. Banerjee, S., Kundu, T. Symmetric and anti-symmetric Rayleigh-Lamb modes in sinusoidally corrugated waveguides // International Journal of Solids and Structures. 2006. 43(21). Pp. 6551-6567. DOI: 10.1016/j.ijsolstr.2006.01.005.

21. Gavric L. Finite element computation of dispersion properties of thin walled waveguides. Journal of Sound and Vibration. 1994. 173 (1). Pp. 113–124
22. Houillon, L., Ichchou, M.N., Jezequel, L. Wave motion in thin walled structures. Journal of Sound and Vibration. 2005. 281(3–5). Pp. 483–507. DOI: 10.1016 / j.jsv.2004.01.020.
23. Antufiev, V.A., Egorova, O.V., Kuznetsova, E.L. Dinamika rebristoy plastini pod deystviem podvijnoy nagruzki [Dinamics of a stiffened plate under moving loads]. Izvestiya TulGU. Technicheskie nauki. 2017. No. 7. Pp. 344–350. (rus)
24. Karpov, V.V., Ignat'ev, O.V., Semenov, A.A. The stress-strain state of ribbed shell structures. Magazine of Civil Engineering. 2017. No.6. Pp. 147–160. DOI: 10.18720/MCE.74.12.
25. Galiyev, Sh.U., Babich, Y.N., Semenov, A.A., Juraxovskiy, S.V., Nechitaylo, N.V., Romashenko, V.A. Chislennoe modelirovanie volnovykh prossessov v ogranichennykh sredax [Numerical Simulation of wave processes in confined media]. Kyiv: Naukova Dumka, 1989. 199 p. (rus)
26. Galiyev, Sh.U. Dinamika gidrouprugoplasticheskikh system [Dinamics of hydroelastoplastic systems]. Kyiv: Naukova Dumka, 1981. 276 p. (rus)
27. Khudoynazarov, K., Abdirashidov, A. Nestatsionarnoe vzaimodeystviye uprugoplasticheski deformiruyemykh elementov konstruksiy s jidkostyu [Nonstatsionary interaction of elastoplastic deformable structural elements with a liquid]. Tashkent: FAN, 2005. 220 p. (rus)
28. Khalmuradov, R., Khudoynazarov, K., Nisnonov, U. Nonlinear vibrations ribbed circular plate under influence of pulse loading. International Journal of Advanced Research in Science, Engineering and Technology. 2018. 5(3). Pp. 5289–5296.

Information about authors:

Rustam Khalmuradov, *Doctor of Technical Science*
E-mail: rustami@list.ru

Khayrulla Khudoynazarov, *Doctor of Technical Science*
ORCID: https://orcid.org/0000-0001-8994-9738
E-mail: khayrullakhudoynazarov@gmail.com

Utkir Nishanov, *PhD*
E-mail: utkirn1978@mail.ru

Received 11.05.2020. Approved after reviewing 26.04.2022. Accepted 12.06.2022.